4-2004

Origin of Cooperativity in the Activation of Fructose-1,6-bisphosphatase by Mg2+

Scott W. Nelson
Iowa State University, swn@iastate.edu

Richard B. Honzatko
Iowa State University, honzatko@iastate.edu

Herbert J. Fromm
Iowa State University

Origin of Cooperativity in the Activation of Fructose-1,6-bisphosphatase by Mg2+

Abstract

Fructose-1,6-bisphosphatase requires a divalent metal cation for catalysis, Mg^{2+}being its most studied activator. Phosphatase activity increases sigmoidally with the concentration of Mg^{2+}, but the mechanistic basis for such cooperativity is unknown. Bound magnesium cations can interact within a single subunit or between different subunits of the enzyme tetramer. Mutations of Asp^{118}, Asp^{121}, or Glu^{97} to alanine inactivate the recombinant porcine enzyme. These residues bind directly to magnesium cations at the active site. Three different hybrid tetramers of fructose-1,6-bisphosphatase, composed of one wild-type subunit and three subunits bearing one of the mutations above, exhibit kinetic parameters (K_m for fructose-1,6-bisphosphate, 1.1–1.8 μM; K_a for Mg^{2+}, 0.34–0.76 mM; K_i for fructose-2,6-bisphosphate, 0.11–0.61 μM; and IC_{50} for AMP, 3.8–7.4 μM) nearly identical to those of the wild-type enzyme. Notwithstanding these similarities, thek_{cat} parameter for each hybrid tetramer is approximately one-fourth of that for the wild-type enzyme. Evidently, each subunit in the wild-type tetramer can independently achieve maximum velocity when activated by Mg^{2+}. Moreover, the activities of the three hybrid tetramers vary sigmoidally with the concentration of Mg^{2+} (Hill coefficients of ~2). The findings above are fully consistent with a mechanism of cooperativity that arises from within a single subunit of fructose-1,6-bisphosphatase.

Keywords

Enzymes, Fructose, Magnesium printing plates, fructose bisphosphatase, glutamic acid

Disciplines

Biochemistry | Chemistry | Molecular Biology

Comments

This article is from *Journal of Biological Chemistry* 279 (2004): 18481, doi: 10.1074/jbc.M308811200. Posted with permission.

THE JOURNAL OF BIOLOGICAL CHEMISTRY
Vol. 279, No. 18, Issue of April 30, pp. 18481–18487, 2004
Printed in U.S.A.

Origin of Cooperativity in the Activation of Fructose-1,6-bisphosphatase by Mg^{2+}*

Received for publication, August 8, 2003, and in revised form, February 20, 2004
Published, JBC Papers in Press, February 20, 2004, DOI 10.1074/jbc.M308811200

Scott W. Nelson, Richard B. Honzatko, and Herbert J. Fromm‡

From the Department of Biochemistry, Biophysics, and Molecular Biology, Iowa State University, Ames, Iowa 50011

Fructose-1,6-bisphosphatase requires a divalent metal cation for catalysis, Mg^{2+} being its most studied activator. Phosphatase activity increases sigmoidally with the concentration of Mg^{2+}, but the mechanistic basis for such cooperativity is unknown. Bound magnesium cations can interact within a single subunit or between different subunits of the enzyme tetramer. Mutations of Asp^{118}, Asp^{121}, or Glu^{97} to alanine inactivate the recombinant porcine enzyme. These residues bind directly to magnesium cations at the active site. Three different hybrid tetramers of fructose-1,6-bisphosphatase, composed of one wild-type subunit and three subunits bearing one of the mutations above, exhibit kinetic parameters (K_m for fructose-1,6-bisphosphate, 1.1–1.8 μM; K_a for Mg^{2+}, 0.34–0.76 mM; K_i for fructose-2,6-bisphosphate, 0.11–0.61 μM; and IC_{50} for AMP, 3.8–7.4 μM) nearly identical to those of the wild-type enzyme. Notwithstanding these similarities, the k_{cat} parameter for each hybrid tetramer is approximately one-fourth of that for the wild-type enzyme. Evidently, each subunit in the wild-type tetramer can independently achieve maximum velocity when activated by Mg^{2+}. Moreover, the activities of the three hybrid tetramers vary sigmoidally with the concentration of Mg^{2+} (Hill coefficients of ~2). The findings above are fully consistent with a mechanism of cooperativity that arises from within a single subunit of fructose-1,6-bisphosphatase.

Fructose-1,6-bisphosphatase (D-fructose-1,6-bisphosphate 1-phosphohydrolase, EC 3.1.3.11; FBPase)[1] catalyzes the hydrolysis of fructose-1,6-bisphosphate ($F16P_2$) to fructose-6-phosphate and inorganic phosphate (P_i) (1, 2). Fructose-2,6-bisphosphate ($F26P_2$) and AMP inhibit FBPase synergistically (3) and can potentially limit throughput of the entire gluconeogenic pathway by their effect on FBPase (4, 5). $F26P_2$ binds at the active site, and AMP binds to an allosteric site remote from any of the active sites of the FBPase tetramer (6). FBPase requires divalent cations (Mg^{2+}, Mn^{2+}, or Zn^{2+}) for catalysis (2, 7). Monovalent cations such as K^+ or NH_4^+ further enhance activity (8, 9). AMP inhibition is cooperative (Hill coefficient of 2) and competitive with respect to divalent metal cations and noncompetitive with respect to substrate (10). Results from fluorescence and crystallography support the mutually exclusive association of AMP and Mg^{2+} with FBPase (11, 12).

Porcine FBPase, the most extensively studied of all of the FBPases, is a homotetramer of subunit molecular mass of 37 kDa (13). It exists in at least two conformational states designated R and T (14, 15). AMP stabilizes the T-state, whereas substrates or products in combination with metal cations favor the R-state. A dynamic loop (residues 52–72) interacts with the active site (engaged conformation), providing one side chain (Asp^{68}) for metal coordination and orienting other side chains (Glu^{97} and Asp^{74}) essential to catalysis (16–22). T-state FBPase (found in the presence of AMP) stabilizes the loop in a conformation withdrawn from the active site (disengaged conformation). Mutations that destabilize the engaged conformation of loop 52–72 reduce FBPase activity and Mg^{2+} affinity, whereas mutations that destabilize the disengaged conformation lessen AMP inhibition without causing significant change to the binding affinity of an AMP analogue for the allosteric site (20).

Equilibrium binding and kinetic experiments are in apparent conflict regarding the stoichiometry and cooperativity of metal cation association with FBPase. Benkovic *et al.* (23) discovered that four Zn^{2+} or Mn^{2+} bind with negative cooperativity to high affinity sites and an additional four metal cations exhibit independent binding to sites of lower affinity. Binding studies of metal activators in the absence of substrate, however, preclude significant interactions between metal cations and the 1-phosphoryl group of $F16P_2$ (12, 16–18). Horecker and colleagues (24) observed positive cooperativity in the binding of Mn^{2+} to high affinity sites and independent binding to sites of low affinity and detected a third class of metal binding sites in the presence of a substrate analog. In contrast, Mg^{2+}-positive cooperativity is unequivocal in the kinetics of FBPase at pH 7 (7) and yet at pH 9.6, Mg^{2+} cooperativity disappears (9).

Cooperativity in Mg^{2+} activation of FBPase can arise in principle from steady-state kinetics or from thermodynamic coupling between metal binding sites. Individual terms for ligand concentrations in the general relationship for a steady-state Random Bi Bi kinetic mechanism are of order two (25). However, second order terms disappear for a Random Bi Bi kinetic mechanism in which all of the rates of transition are fast relative to those governing the interconversion of the ternary substrate- and product-enzyme complexes (rapid-equilib-

* This work was supported in part by National Institutes of Health Research Grant NS 10546. The costs of publication of this article were defrayed in part by the payment of page charges. This article must therefore be hereby marked "*advertisement*" in accordance with 18 U.S.C. Section 1734 solely to indicate this fact.

‡ To whom correspondence should be addressed. Tel.: 515-294-6116; Fax: 515-294-0453; E-mail: hjfromm@iastate.edu.

[1] The abbreviations used are: FBPase, fructose-1,6-bisphosphatase; $F16P_2$, fructose 1,6-bisphosphate; $F26P_2$, fructose 2,6-bisphospate; Glu-tagged, C-terminal extension of the FBPase subunit by 9 glutamic acid residues; wild type:Glu^{97} → Ala (1:3) hybrid tetramer, FBPase composed of one wild-type subunit and three Glu^{97} → Ala Glu-tagged subunits; wild type:Asp^{118} → Ala (1:3) hybrid tetramer, FBPase composed of one wild-type subunit and three Asp^{118} → Ala Glu-tagged subunits; wild type:Asp^{121} → Ala (1:3) hybrid tetramer, FBPase composed of one wild-type subunit and three Asp^{121} → Ala Glu-tagged subunits; HPLC, high pressure liquid chromatography.

rium condition). Hence, the transition from a noncooperative system at pH 9.6 to a cooperative system at pH 7 could be attributed to the departure from rapid-equilibrium kinetics. Mg^{2+} cooperativity could occur then even for a single set of independent binding sites.

If the kinetic mechanism remains rapid-equilibrium at pH 7.5, however, cooperativity in Mg^{2+} activation necessarily comes from the thermodynamic coupling of two or more binding sites for metal cations. Recent crystal structures of the R-state enzyme reveal ordered binding sites for two Mg^{2+} and the binding of a third Mg^{2+} to mutually exclusive third and fourth sites (18). Side chains of Asp^{118} and Glu^{97} coordinate pairs of metal cations, and a phosphoryl species (at the 1-phosphoryl site) coordinates all three metal cations. Hence, crystal structures present several avenues for thermodynamic coupling between metal sites within a subunit.

Coupling between metal sites of different subunits, however, is also a possibility. The two structural domains of the FBPase subunit undergo a 2–3° reorientation as metal cations bind to the active site (16). A metal-induced movement of domains within one subunit could influence the free energy of metal association in neighboring subunits.

Presented here are data that bear directly on Mg^{2+} cooperativity in FBPase. A thorough study of the kinetic mechanism of FBPase at pH 7.5 is fully consistent with rapid-equilibrium kinetics. Mg^{2+} cooperativity then most probably comes from the thermodynamic coupling of metal binding sites. In principle, the functional properties of hybrid oligomeric enzymes can reveal whether coupling occurs between sites of the same subunit or different subunits (26–29). Mutations of residues that directly coordinate metal cations (Asp^{121}, Asp^{118}, or Glu^{97}) inactivate FBPase, and yet hybrid tetramers with one wild-type subunit and three mutant subunits retain Mg^{2+} cooperativity. Results from metal binding, kinetics, and structural studies then are all consistent with intrasubunit coupling of metal binding sites as the basis for Mg^{2+} cooperativity in FBPase.

EXPERIMENTAL PROCEDURES

Materials—$F16P_2$, $F26P_2$, $NADP^+$, and AMP were purchased from Sigma. Glucose-6-phosphate dehydrogenase and phosphoglucose isomerase came from Roche Applied Science. Other chemicals were reagent grade or equivalent. QSW-HR HPLC resin was from Toso-Hass Bioseparations. FBPase-deficient *Escherichia coli* strain DF 657 came from the Genetic Stock Center, Yale University. Plasmids used in the expression of Glu-tagged FBPase came from a previous investigation (28). All of the oligonucleotides came from Sigma.

Mutagenesis of Wild-type FBPase—Specific base changes in double-stranded plasmids employed QuikChange site-directed mutagenesis (Stratagene). Individual mutations of Asp^{121}, Asp^{118}, and Glu^{97} to alanine on the Glu-tagged plasmid were accomplished with primers 5′-GGTCTGTTTTGATCCCCTCGCGGGATCGTCGAACATC-3′, 5′-GGTAAATACGTGGTCTGTTTTGCGCCCCTCGATGGATCG-3′, and 5′-GCGTTCTCGTGTCAGCGGAAGATAAAAACGCC-3′, respectively. Primers for the second mutagenesis reaction are the reverse complements of the forward primers. Results from mutagenesis were confirmed by sequencing the promoter region and the entire open reading frame. The Iowa State University sequencing facility provided DNA sequences using the fluorescent dye-dideoxy terminator method.

Expression and Purification of Wild-type and Mutant Homotetramers—Wild-type and mutant FBPases were expressed in *E. coli* strain DF 657 and purified to homogeneity. Cell-free extracts of the wild-type, wild-type Glu-tagged, and mutant Glu-tagged homotetramers were subjected to heat treatment (65 °C for 5 min) followed by centrifugation. The supernatant fluid was loaded onto a Cibracon Blue-Sepharose column previously equilibrated with 20 mM Tris-HCl, pH 7.5. FBPases were eluted from that column by 5 mM AMP in 20 mM Tris-HCl, pH 7.5. The eluent was loaded directly onto a DEAE-Sepharose column and eluted with a NaCl gradient (0–0.3 M) in 20 mM Tris-HCl, pH 7.5. Wild-type and Glu-tagged enzymes eluted at ~0.1 and 0.25 M NaCl, respectively. Protein purity and concentration was confirmed by SDS-polyacrylamide gel electrophoresis (30) and the Bradford assay (31), respectively.

Formation and Purification of Hybrid Enzymes—Only pure enzymes were used in hybridization procedures. Wild-type and mutant FBPases were combined and incubated overnight at 4 °C, after which the mixture was loaded onto a QSW-HR HPLC column previously equilibrated with 20 mM Tris-HCl, pH 7.5. Individual hybrids were eluted with a NaCl gradient (0–0.3 M) in 20 mM Tris-HCl, pH 7.5. Anion exchange chromatography separated FBPase tetramers by variations in net charge because of the numbers and relative placement of Glu-tagged subunits. Assignment of specific hybrid types to eluted peaks employed methods and considerations described previously (28, 29). Once isolated, hybrid tetramers were maintained at room temperature to retard further subunit exchange. All of the kinetics data were acquired within 2 h of hybrid purification, after which hybrid enzymes were re-examined using native PAGE. These gels confirmed the absence of subunit rearrangement.

Circular Dichroism Spectroscopy—Circular dichroism spectra were recorded for wild type, mutants, and hybrid FBPases at room temperature on a Jasco J710 CD spectrometer using a 1-cm cell and a protein concentration of 0.35 mg/ml. Spectra were collected from 200 to 260 nm in increments of 1.3 nm. Each spectrum, an average of three independent scans, was blank-corrected using the software package provided with the instrument.

Kinetic Experiments—Assays for the determination of specific activity, k_{cat}, and activity ratios at pH 7.5 and 9.5 employed the coupling enzymes, phosphoglucose isomerase, and glucose-6-phosphate dehydrogenase (1). The reduction of $NADP^+$ to NADPH was monitored by absorbance spectroscopy at 340 nm. All of the other assays used the same coupling enzymes but monitored the production of NADPH by fluorescence emission at 470 nm using an excitation wavelength of 340 nm. Assays were performed at room temperature (22 °C). Initial velocities were determined by using the software Igor Pro (Wavemetrics, Inc.).

RESULTS

Kinetic Mechanism of the Wild-type Enzyme—The kinetic mechanism of FBPase was determined at pH 7.5 by the measurement of initial velocities at various concentrations of Mg^{2+} and $F16P_2$. Double reciprocal plots of initial velocity against free $F16P_2$ and Mg^{2+} concentrations (Fig. 1) revealed families of intersecting lines indicative of a sequential mechanism in which the formation of a complete active-site complex must precede the rate-limiting step. Fits of data to functional forms representing a variety of kinetic mechanisms clearly established Equation 1 as the best relationship with the fewest degrees of freedom,

$$v = (V_{max}\cdot A^2\cdot B)/(A^2\cdot B + K_a\cdot B + K_b\cdot A^2 + K_{ia}\cdot K_b) \quad \text{(Eq. 1)}$$

where V_{max}, A, B, K_a, K_b, and K_{ia} represent the maximum velocity of the reaction, the concentration of free Mg^{2+}, the concentration of free $F16P_2$, the Michaelis-Menten constant for Mg^{2+}, the Michaelis-Menten constant for $F16P_2$, and the dissociation constant for Mg^{2+}, respectively. Acceptable fits using data at pH 7.5 require the second order term in the concentration of free Mg^{2+}. Kinetic parameters determined by the fit to Equation 1 are indicated in Table I.

Equation 1 is valid for rapid-equilibrium Random Ter Ter and steady-state Ordered Ter Ter kinetic mechanisms in which two Mg^{2+} bind in a single step (Hill coefficient constrained to two). The response of the system to competitive inhibitors can distinguish between random and ordered mechanisms (32). Cd^{2+} and $F26P_2$ inhibit FBPase competitively with respect to Mg^{2+} (10) and $F16P_2$ (4), respectively. For a random mechanism, the competitive inhibitor of one substrate should be a noncompetitive inhibitor of the other substrate, whereas for an ordered mechanism, the competitive inhibitor of the second substrate should be an uncompetitive inhibitor of the first substrate. The appropriate double reciprocal plots (Fig. 2) clearly indicate noncompetitive inhibition of FBPase by Cd^{2+} and $F26P_2$ with respect to Mg^{2+} and $F16P_2$, respectively, hence

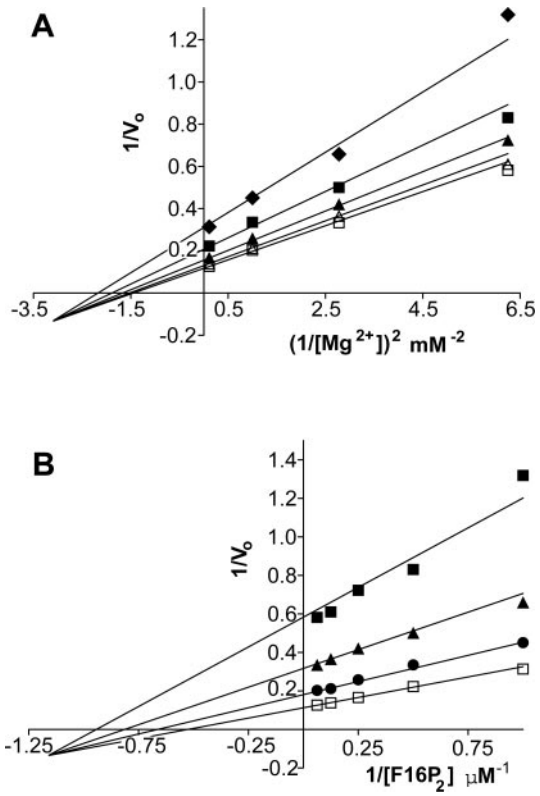

FIG. 1. **Double reciprocal plots indicative of a sequential kinetic mechanism for FBPase.** *A*, plot of reciprocal velocity against $1/[Mg^{2+}]^2$ at fixed free $F16P_2$ concentrations of 1 (♦), 2 (■), 4 (▲), 8 (△), and 20 μM (□). *B*, plot of reciprocal velocity against $1/[F16P_2]$ at fixed free Mg^{2+} concentrations of 0.4 (■), 0.6 (▲), 1 (●), and 3 mM (□). All of the assays were in 50 mM Hepes, pH 7.5, 150 mM KCl, and 0.1 mM EDTA. At pH 7.5, all of the EDTA is complexed by Mg^{2+} and trace heavy metals. The total concentration of trace heavy metals, however, does not exceed 0.1 μM (see the legend to Fig. 2). Hence, the concentration of free Mg^{2+} was taken as the total concentration of Mg^{2+} less the total concentration of EDTA. The concentration of free Mg^{2+} was not corrected for losses because of the formation of Mg^{2+}·$F16P_2$ complexes (K_d ~4 mM, pH 7.5). Such losses vary from 2 to 6 μM under the conditions of assay and are small relative to total concentrations of Mg^{2+}. Trend lines come from Equation 1 using values for parameters listed in Table I.

TABLE I
Values for parameters of Scheme I determined by fits of Equation 1 to the data in Fig. 1

Constant	Enzyme interaction	Value
K_{ia}	$E + 2Mg^{2+} \Leftrightarrow E \cdot (Mg^{2+})_2$	0.35 ± 0.07 mM^2
K_{ib}	$E + F16P_2 \Leftrightarrow E \cdot F16P_2$	0.9 ± 0.2 μM
K_a	$E{\cdot}F16P_2 + 2Mg^{2+} \Leftrightarrow E{\cdot}F16P_2{\cdot}(Mg^{2+})_2$	0.74 ± 0.05 mM^2
K_b	$E{\cdot}(Mg^{2+})_2 + F16P_2 \Leftrightarrow E{\cdot}F16P_2{\cdot}(Mg^{2+})_2$	2.0 ± 0.1 μM

a random mechanism. Data from Fig. 2*a* were fit to a model for linear noncompetitive inhibition as shown in Equation 2,

$$v = (V_{max}{\cdot}A^2{\cdot}B)/\{K_b{\cdot}A^2 + K_{ia}{\cdot}K_b{\cdot}(1 + I/K_{ix}) + A^2{\cdot}B + K_a{\cdot}(1 + I/K_{iix}){\cdot}B\} \quad \text{(Eq. 2)}$$

where V_{max}, A, B, K_a, K_b, and K_{ia} are defined as in Equation 1, I is the concentration of Cd^{2+}, and K_{ix} and K_{iix} are equilibrium constants defined in Table II. In fitting the data of Fig. 2*a*, the concentration of Mg^{2+} (symbolized by A) is fixed, whereas concentrations of $F16P_2$ and Cd^{2+} (symbolized by B and I, respectively) vary. Numerical values for K_a, K_b, and K_{ia} come from Table I. V_{max}, K_{ix}, and K_{iix} are the adjustable parameters with optimized values reported for K_{ix} and K_{iix} in Table II. Data from Fig. 2*b* were fit to a model for linear noncompetitive

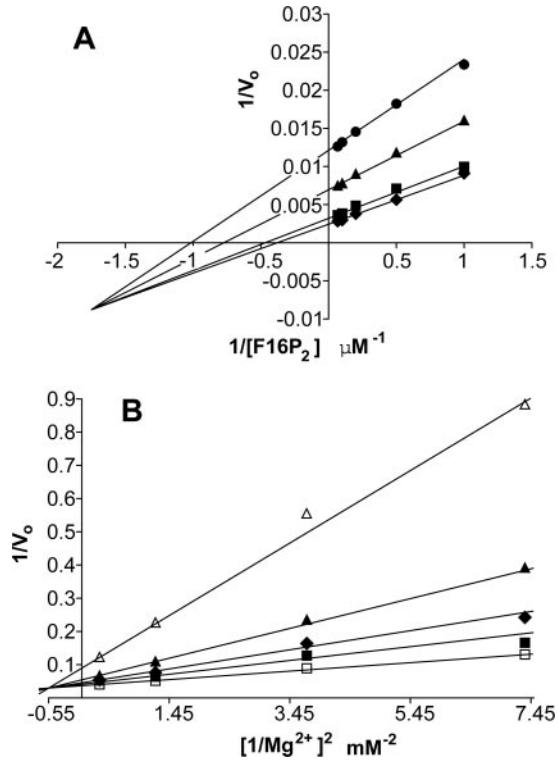

FIG. 2. **Inhibition of FBPase by Cd^{2+} and $F26P_2$.** *A*, plot of reciprocal velocity against $1/[F16P_2]$ at a fixed Mg^{2+} concentration of 5 mM and fixed Cd^{2+} concentrations of 0 (♦), 1 (■), 6 (▲), and 12 μM (●). *B*, plot of reciprocal velocity against $1/[Mg^{2+}]^2$ at a fixed $F16P_2$ concentration of 20 μM and fixed $F26P_2$ concentrations of 0 (□), 0.3 (■), 0.6 (♦), 1.2 (▲), and 3.6 μM (△). Assays were in 50 mM Hepes, pH 7.5, 150 mM KCl, and 0.1 μM EDTA. FBPase achieves maximum activity only in the presence of EDTA (3). EDTA acts either as an allosteric activator of FBPase, or it chelates trace heavy metals that inhibit the enzyme (3). A bound EDTA molecule has not been observed in any crystal structure of FBPase, an observation that supports the latter mechanism. The concentration of EDTA in the experiments of *a* must be small relative to the lowest concentration of Cd^{2+} but sufficient to allow maximum activation of FBPase. A concentration of 0.1 μM EDTA satisfies both conditions. Concentrations of coordination complexes between divalent cations and phosphoryl ligands are negligible under the conditions of assay as evidenced by the close agreement between observed data and trend lines. Trend lines come from Equations 2 and 3 using the parameters listed in Tables I and II.

TABLE II
Constants for the inhibition of FBPase by $F26P_2$ and Cd^{2+} determined by fits of Equations 2 and 3 to the data of Fig. 2

Constant	Equilibrium condition	Value
		*n*M
K_{ix}	$E + Cd^{2+} \Leftrightarrow E{\cdot}Cd^{2+}$	300 ± 100
K_{iix}	$E{\cdot}F16P_2 + Cd^{2+} \Leftrightarrow E{\cdot}F16P_2 \Leftrightarrow Cd^{2+}$	96 ± 5
K_{iy}	$E + F26P_2 \Leftrightarrow E{\cdot}F26P_2$	39 ± 5
K_{iiy}	$E{\cdot}Mg^{2+} + F26P_2 \Leftrightarrow E{\cdot}F26P_2{\cdot}Mg^{2+}$	150 ± 10

inhibition as well as shown in Equation 3,

$$v = (V_{max}{\cdot}A^2{\cdot}B)/\{K_a{\cdot}B + K_{ia}{\cdot}K_b{\cdot}(1 + I/K_{iy}) + A^2{\cdot}B + K_b{\cdot}(1 + I/K_{iiy}){\cdot}A^2\} \quad \text{(Eq. 3)}$$

where V_{max}, A, B, K_a, K_b, and K_{ia} are defined as in Equation 1, I is the concentration of $F26P_2$, and K_{iy} and K_{iiy} are equilibrium constants defined in Table II. For the data of Fig. 2*b*, the concentration of $F16P_2$ (symbolized by B) is fixed, whereas concentrations of Mg^{2+} and $F26P_2$ (symbolized by A and I, respectively) vary. V_{max}, K_{iy} and K_{iiy} are optimized with values assigned to K_a, K_b, and K_{ia} from Table I. Numerical values for K_{iy} and K_{iiy} appear in Table II.

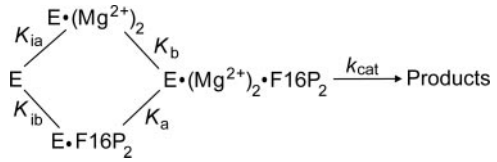

SCHEME 1

A kinetic mechanism that accounts for the data in Figs. 1 and 2 is in Scheme I. All of the steps are in rapid-equilibrium relative to the breakdown of the quaternary $E{\cdot}(Mg^{2+})_2{\cdot}F16P_2$ complex. The data are fully consistent with a rapid-equilibrium Random Ter Ter mechanism, the central complex of which must have at least two magnesium cations.

Expression, Purification, and Secondary Structure of FBPase Constructs—Wild-type and mutant FBPases behaved consistently through purification, becoming at least 95% pure on the basis of SDS-PAGE and native PAGE (data not shown). Furthermore, subunit exchange between wild type and wild-type Glu-tagged homotetramers proceeded at rates identical to those of wild type and mutant Glu-tagged homotetramers ($t_{½}$ = 1 h). Hybrid enzymes eluted over six peaks from HPLC-DEAE chromatography (Fig. 3). Hybrid tetramers with one wild-type subunit and three mutant Glu-tagged subunits (1:3 hybrid enzymes) were resolved by HPLC-DEAE chromatography and native PAGE electrophoresis (Fig. 4). Circular dichroism spectra of wild type, mutant homotetramers, and equilibrium hybrid mixtures are identical from 200 to 260 nm (data not shown), indicating consistent folding and secondary structure for the constructs used here.

Kinetics of Hybrid Enzymes—Hybrid enzymes were used in experiments immediately following their purification. Kinetic parameters for wild type, wild-type Glu-tagged, and 1:3 hybrid enzymes are in Table III. Mutant Glu-tagged homotetramers exhibited no activity over a wide range of assay conditions (pH 7.5–9.5, Mg^{2+} concentrations of up to 50 mM, enzyme concentrations of up to 10 mg/ml, and assay times as long as 10 min). Assay conditions at elevated enzyme concentrations and increased times place an upper limit on the activity of 10^{-7} relative to that of the wild-type enzyme. Wild type and wild-type Glu-tagged homotetramers have virtually identical kinetic parameters. Hybrid enzymes of Ala^{97}, Ala^{118}, and Ala^{121} mutant subunits are 24 ± 6, 18 ± 7, and 26 ± 7%, respectively, as active as wild-type FBPase. Wild-type and hybrid enzymes exhibit similar curves for Mg^{2+} activation (Fig. 5). K_a values for Mg^{2+} decreased no >2-fold for hybrid enzymes relative to that of wild-type FBPase. Hybrid enzymes have Hill coefficients for Mg^{2+} ranging from 1.8 to 2.0. Only the K_i for $F26P_2$ of the wild type:Asp^{121} → Ala (1:3) hybrid tetramer shows significant change, being 5-fold higher than that of the wild-type homotetramer. AMP is a cooperative inhibitor of all 1:3 hybrid tetramers with 4-fold increases in IC_{50} values for the wild-type:Asp^{121} → Ala and wild type:Asp^{118}→ Ala (1:3) hybrid tetramers.

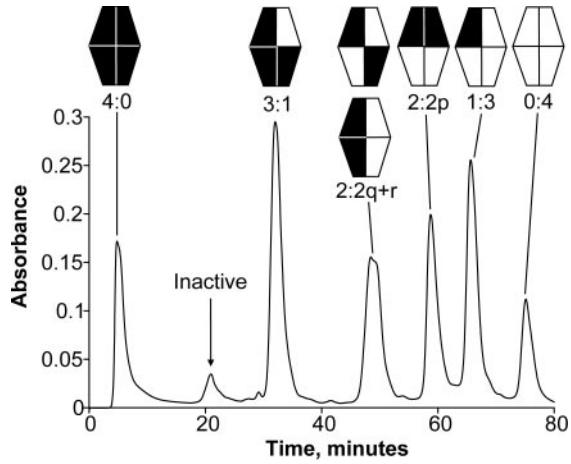

FIG. 3. **Elution profile for the wild type:Asp^{121} → Ala (1:3) hybrid tetramer.** The penultimate peak is the 1:3 hybrid tetramer composed of three Glu-tagged Asp^{121} → Ala subunits (represented as *open polygons* in the stylized FBPase tetramers) and one wild-type subunit (*filled polygon*). Three types of 2:2 hybrid tetramers are possible, distinguished by the relative positions of mutant and wild-type subunits. The 2:2q and 2:2r configurations have mutant Glu-tagged subunits in opposite halves (*top/bottom*) of the FBPase tetramer and cannot be resolved by anion-exchange chromatography. The 2:2p configuration has mutant Glu-tagged subunits in the same half of the tetramer. Peaks in the elution profile are assigned by the procedures of Ref. 28. The peak marked by the *arrow* has no FBPase activity.

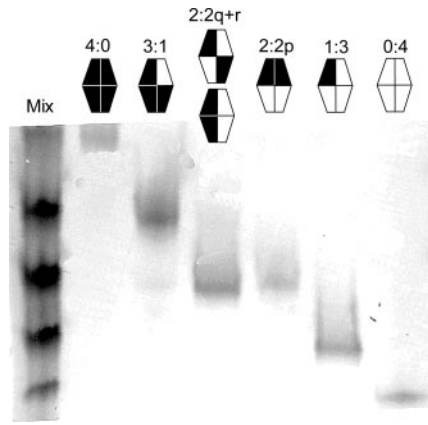

FIG. 4. **Nondenaturing polyacrylamide gel electrophoresis of purified hybrids.** Each lane is labeled for its hybrid composition: *Mix*, equilibrium mixture of wild type and Glu-tagged mutant tetramers; *4:0*, wild-type tetramer; *3:1*, hybrid tetramer with three wild-type subunits and one mutant Glu-tagged subunit; *2:2q+r*, unresolved mixture of tetramers with single mutant Glu-tagged subunits in opposite halves (*top/bottom*) of the FBPase tetramer; *2:2p*, hybrid tetramer with two mutant Glu-tagged subunits in the same half of the tetramer; *1:3*, hybrid tetramer with one wild-type subunit and three mutant Glu-tagged subunits; *0:4*, tetramer with four mutant Glu-tagged subunits. Identification of 1:3 hybrid type is based on its electrophoretic and chromatographic mobilities relative to the complete hybrid mixture as described in Ref. 28.

DISCUSSION

Models of Monod *et al.* (33) and Koshland *et al.* (34) link cooperative phenomena to transitions between conformational states. By all measures, the R-state is the predominant form of FBPase in the absence of ligands. The addition of AMP drives an R- to T-state transition, which probably accounts for AMP cooperativity. However, Mg^{2+}, which is an antagonist of AMP, can only stabilize an enzyme already in the R-state. Hence, the known quaternary transition of FBPase is an unlikely basis for Mg^{2+} cooperativity.

Random two-substrate kinetic mechanisms, however, can exhibit apparent cooperativity as noted in the Introduction. FBPase behaves as a two-substrate system at pH 9.6 (rapid-equilibrium Random Bi Bi kinetic mechanism with one Mg^{2+} and one $F16P_2$ molecule forming a ternary complex with the active site (10)). At pH 7.5, the kinetic mechanism changes, becoming steady-state Random Bi Bi, rapid-equilibrium Random Ter Ter, or steady-state Ordered Ter Ter. Data here eliminate a steady-state Ordered Ter Ter kinetic mechanism and are consistent with a rapid-equilibrium Random Ter Ter mechanism. Kinetic data alone, however, cannot exclude a steady-state Random Bi Bi mechanism. Nonetheless, metal binding studies (23, 24) and recent crystal structures of product complexes (16–18) favor multiple binding sites for metal cations. The rapid-equilibrium Random Ter Ter mechanism requires

TABLE III
Kinetic parameters for wild-type, Glu-tagged, and 1:3 hybrid FBPases
Assays employed 0.1 mM EDTA. The concentration of free Mg^{2+} is taken as the total concentration of Mg^{2+} less the total concentration of EDTA.

FBPase	Activity ratio[a]	k_{cat}[b]	K_m-$F16P_2$[c]	K_a-Mg^{2+}[d]	Hill coefficient for Mg^{2+}	K_i-$F26P_2$[c]	IC_{50}-AMP[e]
		sec^{-1}	μM	mM^2		μM	μM
Wild type	3.3	22 ± 1	1.8 ± 0.1	0.67 ± 0.04	1.9 ± 0.1	0.12 ± 0.01	1.6 ± 0.1
Wild-type Glu-tagged	3.5	23 ± 1	2.2 ± 0.1	0.65 ± 0.05	2.1 ± 0.1	0.11 ± 0.01	1.4 ± 0.1
Wild type:$Glu^{97} \rightarrow$ Ala (1:3)	3.2	5.3 ± 0.2	1.8 ± 0.1	0.76 ± 0.07	1.9 ± 0.1	0.16 ± 0.01	3.8 ± 0.2
Wild type:$Asp^{118} \rightarrow$ Ala (1:3)	3.3	3.9 ± 0.2	1.3 ± 0.1	0.32 ± 0.04	2.0 ± 0.1	0.17 ± 0.01	6.9 ± 0.4
Wild type:$Asp^{121} \rightarrow$ Ala (1:3)	3.1	5.8 ± 0.3	1.1 ± 0.1	0.34 ± 0.05	1.8 ± 0.1	0.61 ± 0.04	7.4 ± 0.2

[a] Ratio of specific activities at pH 7.5 and 9.5.
[b] Assays employed saturating [Mg^{2+}] (5 mM) and [$F16P_2$] (20 μM).
[c] Assays used saturating [Mg^{2+}] (5 mM).
[d] Assays used saturating [$F16P_2$] (20 μM).
[e] Assays used fixed [Mg^{2+}] = K_a-Mg^{2+} and saturating [$F16P_2$] (20 μM).

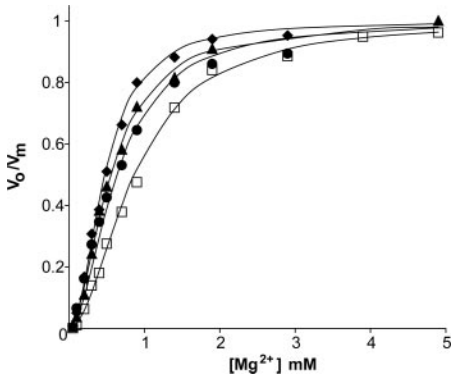

FIG. 5. **Activity of wild-type and hybrid enzymes as a function of free Mg^{2+} concentration.** Curves represent wild-type enzyme (●) and 1:3 hybrid tetramers of wild type and Glu-tagged, $Asp^{118} \rightarrow$ Ala (♦), $Asp^{121} \rightarrow$Ala (▲), and $Glu^{97} \rightarrow$Ala (□) subunits. All of the assays are in 50 mM Hepes, pH 7.5, 150 mM KCl, 0.1 mM EDTA, and 20 μM $F16P_2$. Concentrations of free Mg^{2+} range from 0.1 to 5.0 mM. Determination of free Mg^{2+} concentrations follows the procedure in the legend to Fig. 1.

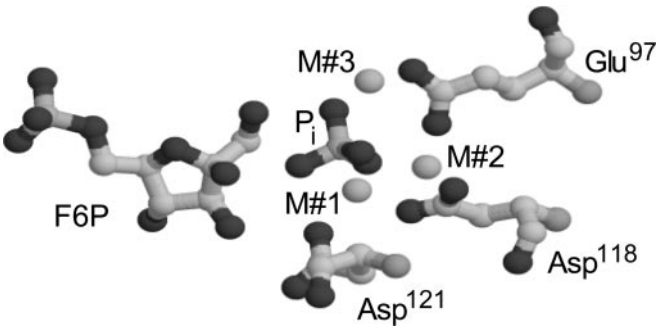

FIG. 6. **Relationship of Asp^{121}, Asp^{118}, and Glu^{97} to the three principal sites of metal coordination in FBPase.** The illustration comes from the three Mg^{2+} complex at pH 7 (Protein Data Bank accession number 1NUY).

multiple metal binding sites, whereas the steady-state Random Bi Bi mechanism allows only a single metal binding site. Of the kinetic mechanisms considered here, only the rapid-equilibrium Random Ter Ter scheme accounts for the full spectrum of data from kinetics, equilibrium binding, and structural studies.

Mg^{2+} and $F16P_2$ interactions with the enzyme are not synergistic as evidenced by the kinetic data. Individual curves in Fig. 1 converge below the *x* axis, indicating higher values for Michaelis-Menten constants (K_a and K_b in Scheme I) than for dissociation constants (K_{ia} and K_{ib}). The presence of the first ligand could sterically hinder the binding of the second ligand. Alternatively, both ligands in combination may divert binding energy to promote the transition state, as for instance, a conformational change in loop 52–72 to its engaged conformation. $F26P_2$ binds also with lower affinity in the presence of Mg^{2+} than in its absence (10). Because the concentration of Mg^{2+} *in vivo* is constant and high enough to completely saturate the enzyme, the Michaelis-Menten constant of $F16P_2$ (K_b in Scheme I) may reflect substrate affinity more accurately than the dissociation constant (K_{ib}). By similar reasoning, K_{iiy} may better represent the affinity of $F26P_2$ for FBPase *in vivo* than does K_{iy}.

Unlike Mg^{2+}, Cd^{2+} binds synergistically with $F16P_2$. Cd^{2+} has a higher affinity for the E·$F16P_2$ complex than for the enzyme alone. Cd^{2+} inhibits the enzyme without cooperativity, consistent with independent binding to a single set of sites. The larger size of Cd^{2+} relative to Mg^{2+} runs contrary to steric conflict as an explanation for Mg^{2+}-$F16P_2$ antagonism; however, if Cd^{2+} and $F16P_2$ together cannot divert free energy to promote conformational change (movement of loop 52–72 perhaps), then what appears as binding antagonism for Mg^{2+} and $F16P_2$ could become binding synergism for Cd^{2+} and $F16P_2$.

Asp^{121} coordinates Mg^{2+} at site 1, Asp^{118} coordinates Mg^{2+} at sites 1 and 2, and Glu^{97} coordinates Mg^{2+} at sites 2 and 3 (Fig. 6). The absence of measurable turnover for the Ala^{118}, Ala^{121}, and Ala^{97} mutant proteins is consistent then with the essential role played by divalent cations in FBPase activity. By way of comparison, the Ala^{121} mutation of rat liver FBPase causes a 50,000-fold reduction in activity (35). Reasons for the discrepancy between Ala^{121} FBPases from rat and pig are unclear; however, even a relative activity (mutant *versus* wild-type enzyme) as high as 10^{-3} is insignificant in relation to the ~25% relative activity of the 1:3 hybrid tetramers studied here.

Intersubunit coupling is a favored explanation for Mg^{2+} cooperativity in FBPase kinetics (7), even though no direct evidence supports such a mechanism to the exclusion of other possibilities. Mutations here disrupt all of the possible interactions between metal sites of different subunits, and yet all of the 1:3 hybrid enzymes retain Mg^{2+} cooperativity. The latter infers a coupling mechanism between metal sites within a single subunit. However, which of the metal binding sites are coupled? One site has a high affinity for metal, requiring 2 weeks of dialysis to completely remove divalent cations from it (23). Crystals of FBPase grown in the presence of AMP and Mg^{2+} retain metal only at site 1 (12). Hence, site 1 is the only reasonable candidate for the high affinity binding site for divalent cations. Moreover, for all of the concentrations of Mg^{2+} employed in assays, the metal cation may fully occupy site 1, eliminating it from consideration in cooperative phenomenon. To observe a Hill coefficient of two, sites 2 and 3 must be coupled and, in crystal structures with Mg^{2+} at neutral pH, Glu^{97} bridges metal cations at sites 2 and 3 (17, 18). In a crystal structure at pH 9, Glu^{97} coordinates metals at sites 1 and 2 and a third metal occupies mutually exclusive sites 3 and 4. The loss of Glu^{97} to site 3 is in harmony with the loss of Mg^{2+} cooperativity in FBPase kinetics above pH 9. If FBPase can generate metaphosphate in its active site, as recent evidence

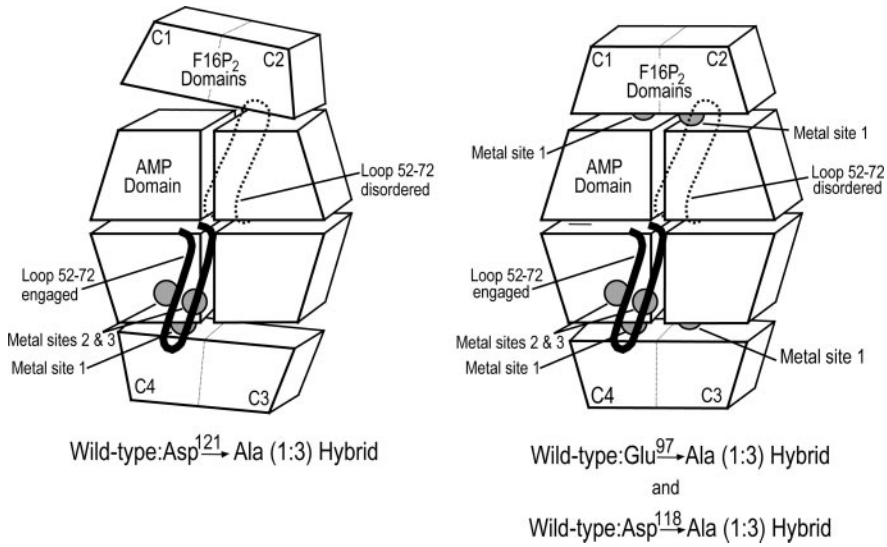

FIG. 7. **Proposed explanation for the 5-fold increase in $F26P_2$ inhibition of the wild type:Asp^{121} → Ala (1:3) hybrid enzyme.** The loss of Asp^{121} eliminates metal binding to site 1. This is the only metal site that bridges the AMP and $F16P_2$ domains of a subunit. The loss of metal from site 1 causes the mis-orientation of $F16P_2$ domains relative to AMP domains in the three mutant subunits of the wild type:Asp^{121} → Ala (1:3) hybrid enzyme (*left*). This disorganized tetramer binds $F26P_2$ with a lower affinity. In contrast, the loss of Glu^{97} or Asp^{118} should have only a modest impact on metal binding to site 1. Hence, in the wild type:Glu^{97} → Ala (1:3) and wild type:Asp^{118} → Ala (1:3) hybrid enzymes, the tetramer retains a high level of structural order and $F26P_2$ inhibition is unimpaired.

suggests (18), a hydroxide ion (the concentration of which in bulk solvent is a 100-fold higher at pH 9.5 than at 7.5) could react without the benefit of a metal cation at site 3. Mutagenesis experiments are in agreement with the analysis above. Mutations of Asn^{64} and Asp^{68}, residues that make up part of metal site 3, or mutations within the loop 52–72 lower the pH 7.5/9.5 activity ratio, decrease Mg^{2+} affinity, and reduce or eliminate Mg^{2+} cooperativity (19, 20). Additionally, the mutation of Arg^{276}, a residue near metal site 3, eliminates Mg^{2+} cooperativity (36), most probably by destabilizing the engaged conformation of loop 52–72 (16).

Although 1:3 hybrid FBPases evidently exclude site coupling between subunits as a basis for Mg^{2+} cooperativity, the 5-fold increase in the K_i for $F26P_2$ exhibited by the wild type:Asp^{121} → Ala (1:3) hybrid enzyme implies some mechanism of coupling between the $F26P_2$ binding site and metal sites 1 in neighboring subunits (Fig. 7). Site 1 differs in at least one respect from other metal sites. Side chains from both the $F16P_2$ and AMP binding domains of the FBPase subunit coordinate the site 1 metal, whereas sites 2 and 3 lie entirely within the AMP domain. The relative orientation of the AMP and $F16P_2$ domains differs by 2–3° between metal-free and metal-product complexes of R-state FBPase (16). This 2–3° re-orientation of domains was originally attributed to the R- to T-state transition (14), but superpositions of subunits from T-state and R-state complexes of FBPase with bound metals show no domain re-orientation (12, 16). Furthermore, the two $F16P_2$ domains of a C1–C2 subunit pair have fixed orientations with respect to each other, a consequence of numerous bridging salt links and hydrogen bonds. (Arg^{243} from subunit C1, for instance, hydrogen bonds with the 6-phosphoryl group of the substrate in subunit C2). Hence, the binding or loss of metal at site 1 in one subunit should affect the neighboring subunit in the C1–C2 pair. This coupling mechanism, however, has no effect on the kinetics of wild-type FBPase, probably because divalent cations always saturate site 1 in assays.

What is unexpected in the functional properties of the wild type:Asp^{121} → Ala (1:3) hybrid enzyme is not necessarily the 5-fold increase in the K_i for $F26P_2$ but the absence of any effect on the K_b for $F16P_2$. Significant differences in the effect of mutations on kinetic parameters for $F16P_2$ and $F26P_2$, however, are not unprecedented. The mutation of Arg^{243} or Lys^{274} to alanine increases the K_i for $F26P_2$ by 1000-fold but increases the K_b for $F16P_2$ only modestly (10–20-fold) (37, 38). Clearly, FBPase recognizes $F16P_2$ and $F26P_2$ differently, but from a structural perspective, these differences are not yet fully understood.

The results presented here support a mechanism in which the metal at site 1 remains bound throughout the catalytic cycle of FBPase and metals at sites 2 and 3 are solely responsible for cooperativity. This three-metal system is consistent with crystal structures of product complexes of FBPase (16–18). Moreover, several different phosphatase enzymes, for instance, alkaline phosphatase, phospholipase C, and the bifunctional enzyme inositol manophosphatase/FBPase from *Methanococcus jannaschii*, may employ similar mechanisms (39–41). Further examination of the human inositol monophosphatase catalytic mechanism suggests that it too uses a three-metal mechanism (41). The three-metal mechanism then may be broadly applicable to enzymes that cleave phosphate esters.

REFERENCES

1. Benkovic, S. T., and de Maine, M. M. (1982) *Adv. Enzymol. Relat. Areas Mol. Biol.* **53,** 45–82
2. Tejwani, G. A. (1983) *Adv. Enzymol. Relat. Areas Mol. Biol.* **54,** 121–194
3. Pilkis, S. J., El-Maghrabi, M. R., McGrane, M. M., Pilkis, J., and Claus, T. H. (1981) *J. Biol. Chem.* **256,** 3619–3622
4. Van Schaftingen, E. (1987) *Adv. Enzymol. Relat. Areas Mol. Biol.* **59,** 45–82
5. Pilkis, S. J., El-Maghrabi, M. R., and Claus, T. H. (1988) *Ann. Rev. Biochem.* **57,** 755–783
6. Xue, Y., Hung, S., Liang, J.-Y., Zhang, Y., and Lipscomb, W. N. (1994) *Proc. Natl. Acad. Sci. U. S. A.* **91,** 12483–12486
7. Nimmo, H. G., and Tipton, K. F. (1975) *Eur. J. Biochem.* **58,** 567–574
8. Nakashima, K., and Tuboi, S. (1976) *J. Biol. Chem.* **251,** 4315–4321
9. Zhang, R., Villeret, V., Lipscomb, W. N., and Fromm, H. J. (1995) *Biochemistry* **35,** 3038–3043
10. Liu, F., and Fromm, H. J. (1990) *J. Biol. Chem.* **265,** 7401–7406
11. Scheffler, J. E., and Fromm, H. J. (1986) *Biochemistry* **25,** 6659–6665
12. Choe, J.-Y., Fromm, H. J., and Honzatko, R. B. (2000) *Biochemistry* **39,** 8565–8574
13. Stone, S. R., and Fromm, H. J. (1980) *Biochemistry* **19,** 620–625
14. Ke, H., Liang, J.-Y., Zhang, Y., and Lipscomb, W. N. (1991) *Biochemistry* **30,** 4412–4420
15. Liu, F., and Fromm, H. J. (1988) *J. Biol. Chem.* **19,** 9122–9128
16. Choe, J.-Y., Poland, B. W., Fromm, H. J., and Honzatko, R. B. (1998) *Biochemistry* **37,** 11441–11450
17. Choe, J.-Y., Nelson, S. W., Fromm, H. J., and Honzatko, R. B. (2003) *J. Biol. Chem.* **278,** 166008–166014
18. Choe, J.-Y., Iancu, C. V., Fromm, H. J., and Honzatko, R. B. (2003) *J. Biol. Chem.* **278,** 166015–166020
19. Kurbanov, F. T., Choe, J.-Y., Honzatko, R. B., and Fromm, H. J. (1998) *J. Biol. Chem.* **273,** 17511–17516
20. Nelson, S. W., Choe, J.-Y., Honzatko, R. B., and Fromm, H. J. (2000) *J. Biol. Chem.* **275,** 29986–29992
21. Nelson, S. W., Iancu, C. V., Choe, J.-Y., Honzatko, R. B., and Fromm, H. J. (2000) *Biochemistry* **39,** 11100–11106
22. Nelson, S. W., Kurbanov, F. T., Honzatko, R. B., and Fromm, H. J. (2001) *J. Biol. Chem.* **276,** 6119–6124
23. Benkovic, P. A., Caperelli, C. A., de Maine, M., and Benkovic, S. J. (1978) *Proc. Natl. Acad. Sci. U. S. A.* **75,** 2185–2189
24. Pontremoli, S., Sparatore, B., Salamino, F., Melloni, E., and Horecker, B. L. (1979) *Arch. Biochem. Biophys.* **194,** 481–485
25. Fromm, S. J., and Fromm, H. J. (1999) *Biochem. Biophys. Res. Commun.* **265,**

448–452
26. Gibbons, I., Ritchey, J. M., and Schachman, H. K. (1976) *Biochemistry* **15,** 1324–1330
27. Fushinobu, S., Kamata, K., Iwata, S., Sakai, H., Ohta, T., and Matsuzawa, H. J. (1996) *J. Biol. Chem.* **271,** 25611–25616
28. Nelson, S. W., Honzatko, R. B., and Fromm, H. J. (2002) *J. Biol. Chem.* **277,** 15539–15545
29. Nelson, S. W., Honzatko, R. B., and Fromm, H. J. (2001) *FEBS Lett.* **492,** 254–258
30. Laemmli, U. K. (1970) *Nature* **227,** 680–685
31. Bradford, M. M. (1976) *Anal. Biochem.* **72,** 248–252
32. Fromm, H. J. (1979) *Methods Enzymol.* **63,** 467–486
33. Monod, J., Wyman, J., and Changeux, J.-P. (1965) *J. Mol. Biol.* **12,** 88–118
34. Koshland, D. E., Jr., Nemethy, G., and Filmer, D. (1966) *Biochemistry* **5,** 365–385
35. El-Maghrabi, M. R., Gidh-Jain, M., Austin, L. R., and Pilkis, S. J. (1993) *J. Biol. Chem.* **268,** 9466–9472
36. Zhang, R., and Fromm, H. J. (1995) *Biochemistry* **34,** 8190–8195
37. Giroux, E., Williams, M. K., and Kantrowitz, E. R. (1994) *J. Biol. Chem.* **269,** 31404–31409
38. El-Maghrabi, M. R., Austin, L. R., Correia, J. J., and Pilkis, S. J. (1992) *J. Biol. Chem.* **267,** 6526–6530
39. Stec, B., Holtz, K. M., and Kantrowitz, E. R. (2000) *J. Mol. Biol.* **299,** 1303–1311
40. Hough, E., Hansen, L. K., Birknes, B., Jynge, K., Hansen, S., Hordvik, A., Little, C., Dodson, E., and Derewenda, Z. (1989) *Nature* **338,** 357–3607
41. Johnson, K. A., Chen, L., Yang, H., Roberts, M. F., and Stec, B. (2001) *Biochemistry* **40,** 618–630

Origin of Cooperativity in the Activation of Fructose-1,6-bisphosphatase by Mg^{2+}

Scott W. Nelson, Richard B. Honzatko and Herbert J. Fromm

J. Biol. Chem. 2004, 279:18481-18487.
doi: 10.1074/jbc.M308811200 originally published online February 20, 2004
